symmetry

MDPI

Article

Quantum Behavior of a $\mathcal{PT}$-Symmetric Two-Mode System with Cross-Kerr Nonlinearity

Jan Peřina Jr. [1,*] **and Antonín Lukš** [2]

[1] Joint Laboratory of Optics, Institute of Physics of the Czech Academy of Sciences, 17. listopadu 50a, 771 46 Olomouc, Czech Republic
[2] Joint Laboratory of Optics, Faculty of Science, Palacký University, 17. listopadu 12, 771 46 Olomouc, Czech Republic
* Correspondence: jan.perina.jr@upol.cz

Received: 12 July 2019 ; Accepted: 31 July 2019; Published: 7 August 2019

Abstract: Quantum behavior of two oscillator modes, with mutually balanced gain and loss and coupled via linear coupling (including energy conserving as well as energy non-conserving terms) and nonlinear cross-Kerr effect, is investigated. Stationary states are found and their stability analysis is given. Exceptional points for $\mathcal{PT}$-symmetric cases are identified. Quantum dynamics treated by the model of linear operator corrections to a classical solution reveals nonclassical properties of individual modes (squeezing) as well as their entanglement.

Keywords: nonlinearly coupled oscillators; PT symmetry; cross-Kerr nonlinearity; stability analysis; quantum properties

1. Introduction

$\mathcal{PT}$-symmetric systems, which contain gain and loss in mutual balance, have been extensively analyzed in various configurations and from different points of view since the pioneering work by Bender and Boettcher occurred [1–3]. The simplest system is composed of two linearly coupled oscillator modes, one exhibiting gain and the other loss [4]. In real physical applications, there occur additional nonlinear Kerr-type terms in both oscillator modes. They originate in physical models of mode amplification and attenuation typically realized via two-level atoms [5]. These models were developed and extensively discussed in the semiclassical and quantum theories of lasers [6]. Stationary states then occur in such systems due to this nonlinearity. The simplest model of two coupled nonlinear oscillator modes has been generalized to include more oscillators in various configurations. The obtained models were applied in many areas of physics including optical coupled structures [7–10], optical waveguides [11,12], coupled optical micro-resonators [13–15], optical lattices [16–19], opto-mechanical systems [20,21], etc.

Recently, attention has been devoted to the consistent quantum description of $\mathcal{PT}$-symmetric systems. To guarantee the validity of commutation relations among the field operators during the evolution, the fluctuating quantum Langevin forces with specific properties have to be considered in the system [22–25]. As a consequence, the noise in the system constantly increases during the evolution both owing to the amplification and attenuation [24]. Despite this, quantum $\mathcal{PT}$-symmetric systems exhibit interesting and appealing features, such as enhancement of interactions around and at exceptional points (EPs) [26] or quantum Zeno effect [27]. The enhancement of nonlinear interactions then opens the door for the generation of nonclassical light (squeezing) and entangled states [28–31].

Here, we investigate the behavior of a specific form of the model of two coupled oscillator modes with amplification and attenuation that includes only the cross-Kerr nonlinear term. In addition, linear coupling of both modes through $\chi^{(2)}$ parametric interaction that does not conserve energy,

is considered [32,33]. It adds or removes photons simultaneously in both modes. This coupling leads to nonclassical properties of the fields and the occurrence of entanglement between the modes [22,32,34], together with the cross-Kerr nonlinear coupling [35,36]. The cross-Kerr coupling is known to play a significant role in quantum non-demolition measurement [37], generation of the states defined in finite-dimensional Hilbert spaces [38] and generation of maximally entangled Bell-type states [39,40]). In general, the cross-Kerr coupling appearing in the so-called Kerr couplers considerably changes their quantum properties [41–43]. The cross-Kerr nonlinearity can even enhance the usual Kerr effect, e.g., when squeezing effects are analyzed [44].

We show that continuous sets of stationary states occur in the model and we analyze their stability. Then, in the framework of the model of quantum superposition of signal and noise [22], we address squeezed-state generation and generation of entangled states around the stationary states. We note that if one of the oscillator modes in the analyzed model attains an additional Kerr nonlinear term, only the trivial stationary states exist. On the other hand, if the standard Kerr nonlinear terms are attributed to both oscillator modes, the system behavior considerably changes and only discrete stationary states are found [45]. We note that related systems were analyzed from the point of view of squeezed-state generation in [29] (without parametric interaction) and [31] (no Kerr terms, parametric interaction in individual modes) and quantum-noise generation [25] (without parametric interaction). In addition, the work [46], where breaking of the oscillatory regime in a classical two-mode $\mathcal{PT}$-symmetric system with the Kerr nonlinearity due to larger modes intensities is reported, is worth mentioning.

The paper is organized as follows. In Section 2, the analyzed system is defined and the corresponding Heisenberg equations are given. Stationary states and their stability are investigated in Section 3. Nonclassical properties of the evolving states are discussed in Section 4. Section 5 presents conclusions.

2. Quantum Hamiltonian and Dynamical Equations

Introducing annihilation ($\hat{a}_j$) and creation ($\hat{a}_j^\dagger$) operators of photons for oscillator modes 1 ($j = 1$) and 2 ($j = 2$) with identical frequencies ω, the considered system is described by the following interaction Hamiltonian $\hat{H}$ [22]:

$$\hat{H} = -i\gamma_1 \hat{a}_1^\dagger \hat{a}_1 - i\gamma_2 \hat{a}_2^\dagger \hat{a}_2 + \left[\epsilon \hat{a}_1^\dagger \hat{a}_2 + \kappa \hat{a}_1 \hat{a}_2 + \text{h.c.}\right] + \beta_c \hat{a}_1^\dagger \hat{a}_2^\dagger \hat{a}_1 \hat{a}_2. \tag{1}$$

We assume that mode 1 is attenuated $\gamma_1 \geq 0$ and mode 2 is amplified $\gamma_2 \leq 0$. Transfer of energy in the system is described by linear coupling constants ϵ and κ. Whereas the coupling constant ϵ characterizes transfer of energy between the modes, the constant κ quantifies energy inserted and removed to/from both modes in the same amount in the $\chi^{(2)}$ parametric process. The nonlinear coupling constant β_c characterizes in Equation (1) the cross-Kerr nonlinear term that is responsible for the occurrence of stationary states. Both $\chi^{(2)}$ term of parametric interaction and cross-Kerr term occur together in nonlinear photonic structures [33] (waveguides, nonlinear fibers). Symbol h.c. replaces the Hermitian conjugated terms.

The Hamiltonian $\hat{H}$ in Equation (1) attains its $\mathcal{PT}$-symmetric form provided that the constants γ_1, γ_2, ϵ, κ and β_c are real and

$$\gamma_1 = -\gamma_2 \equiv \gamma \geq 0. \tag{2}$$

Moreover, to allow for simple physical interpretation, $\mathcal{PT}$-symmetric Hamiltonians are usually applied for the range of parameters in which their linear parts are endowed with real eigenvalues. For the Hamiltonian $\hat{H}$ in Equation (1), this occurs provided that

$$\epsilon^2 - \kappa^2 - \gamma^2 \geq 0. \tag{3}$$

Points in the space of parameters for which equality in Equation (3) holds identify systems with specific properties. They are called exceptional points (EPs) [1]. Without the loss of generality, we further assume $\epsilon > 0$ and $\kappa \geq 0$.

Applying the canonical commutation relations for field operators [5] we obtain the Heisenberg equations from the Hamiltonian $\hat{H}$ in Equation (1),

$$\begin{aligned} \frac{d\hat{a}_1}{dt} &= -\gamma_1\hat{a}_1 - i\epsilon\hat{a}_2 - i\kappa\hat{a}_2^\dagger - i\beta_c\hat{a}_2^\dagger\hat{a}_2\hat{a}_1 + \hat{l}_1, \\ \frac{d\hat{a}_2}{dt} &= -\gamma_2\hat{a}_2 - i\epsilon\hat{a}_1 - i\kappa\hat{a}_1^\dagger - i\beta_c\hat{a}_1^\dagger\hat{a}_1\hat{a}_2 + \hat{l}_2, \end{aligned} \tag{4}$$

and the Hermitian-conjugated ones. The fluctuating Langevin operator forces $\hat{l}_1$ and $\hat{l}_2$ are introduced in Equation (4) in relation to attenuation in mode 1 and amplification in mode 2, respectively. Their properties [22,23,25],

$$\begin{aligned} \langle\hat{l}_1^\dagger(t)\hat{l}_1(t')\rangle = 0, \quad \langle\hat{l}_1(t)\hat{l}_1^\dagger(t')\rangle = 2\gamma_1\delta(t-t'), \\ \langle\hat{l}_2^\dagger(t)\hat{l}_2(t')\rangle = -2\gamma_2\delta(t-t'), \quad \langle\hat{l}_2(t)\hat{l}_2^\dagger(t')\rangle = 0, \end{aligned} \tag{5}$$

guarantee validity of the commutation relations for the field operators during the evolution. In mode 1, they express the fluctuation-dissipation theorem [47,48] according to which any dissipation of the energy from a system has to be accompanied by back-action from the environment. In analogy, in mode 2, the Langevin forces represent a part of the 'fluctuation-amplification theorem' that occurs as a consequence of consistent adding the energy into the system [6]. Symbol δ means the Dirac function.

3. Stationary States and Their Stability

First, we address the Heisenberg equations in Equation (4) in their 'classical' noiseless limit, i.e., we write them for the coherent states $|\alpha_j\rangle$ with complex amplitudes $\alpha_j = \varrho_j \exp(i\varphi_j)$, $j = 1, 2$:

$$\frac{d\varrho_1}{dt} = -\gamma_1\varrho_1 + [\epsilon\sin(\varphi) - \kappa\sin(\psi)]\,\varrho_2, \tag{6}$$

$$\frac{d\varrho_2}{dt} = -\gamma_2\varrho_2 - [\epsilon\sin(\varphi) + \kappa\sin(\psi)]\,\varrho_1, \tag{7}$$

$$\frac{d\varphi_1}{dt} = -[\epsilon\cos(\varphi) + \kappa\cos(\psi)]\,\frac{\varrho_2}{\varrho_1} - \beta_c\varrho_2^2, \tag{8}$$

$$\frac{d\varphi_2}{dt} = -[\epsilon\cos(\varphi) + \kappa\cos(\psi)]\,\frac{\varrho_1}{\varrho_2} - \beta_c\varrho_1^2. \tag{9}$$

In Equations (6) and (7), we suitably replace the phases φ_1 and φ_2 by their sum $\psi = \varphi_2 + \varphi_1$ and difference $\varphi = \varphi_2 - \varphi_1$.

To reveal the stationary complex amplitudes α_1 and α_2, we set the time derivatives in Equations (6)–(9) to zero. Before analyzing the obtained equations in detail, we note that there exist the trivial stationary states with $\varrho_1^{\mathrm{st}} = \varrho_2^{\mathrm{st}} = 0$ and arbitrary values of phases φ_1^{st} and φ_2^{st}. Under the stationary conditions, Equations (8) and (9) for the phases φ_1 and φ_2 are dependent and, e.g., Equation (8) gives us:

$$\varrho_1^{\mathrm{st}}\varrho_2^{\mathrm{st}} = -(\mathrm{c}_\epsilon + \mathrm{c}_\kappa)/\beta_c. \tag{10}$$

To simplify the notation, we use in Equation (10) and below the following functions that substitute the phases ψ and φ:

$$\mathrm{s}_\epsilon = \epsilon\sin(\varphi^{\mathrm{st}}), \quad \mathrm{c}_\epsilon = \epsilon\cos(\varphi^{\mathrm{st}}), \quad \mathrm{s}_\kappa = \kappa\sin(\psi^{\mathrm{st}}), \quad \mathrm{c}_\kappa = \kappa\cos(\psi^{\mathrm{st}}). \tag{11}$$

Furthermore, the coupled Equations (6) and (7) considered to be functions of ϱ_1^{st} and ϱ_2^{st} have a nontrivial solution provided that their determinant is zero:

$$\mathrm{s}_\epsilon^2 - \mathrm{s}_\kappa^2 + \gamma_1\gamma_2 = 0. \tag{12}$$

Equation (6) when combined with Equation (10) gives us the stationary solution for amplitudes:

$$\varrho_{1,2}^{\mathrm{st}} = \sqrt{\frac{\gamma_{2,1}}{\beta_c}\frac{\mathrm{c}_\epsilon + \mathrm{c}_\kappa}{\pm\mathrm{s}_\epsilon + \mathrm{s}_\kappa}}. \tag{13}$$

According to Equations (12) and (13), one phase, e.g., ψ^{st} in the stationary solution is free. The other phase, φ^{st}, has to fulfill Equation (12) that admits in general four solutions. The amplitudes $\varrho_{1,2}^{\mathrm{st}}$ determined by Equation (13) have to be real and also Equation (10) has to give nonnegative $\varrho_1^{\mathrm{st}}\varrho_2^{\mathrm{st}}$.

To address stability of the stationary solution, we derive the linearized equations for deviations $\delta\varrho_1$, $\delta\varrho_2$, $\delta\varphi$ and $\delta\psi$ from their corresponding stationary values ϱ_1^{st}, ϱ_2^{st}, φ^{st}, and ψ^{st}:

$$\frac{d}{dt}\begin{bmatrix}\delta\varrho_1\\ \delta\varrho_2\\ \delta\varphi\\ \delta\psi\end{bmatrix} = \begin{bmatrix}-\gamma_1 & s_\epsilon - s_\kappa & c_\epsilon\varrho_2^{\mathrm{st}} & -c_\kappa\varrho_2^{\mathrm{st}}\\ -s_\epsilon - s_\kappa & -\gamma_2 & -c_\epsilon\varrho_1^{\mathrm{st}} & -c_\kappa\varrho_1^{\mathrm{st}}\\ G^+ & H^+ & I^+ s_\epsilon & I^+ s_\kappa\\ G^- & H^- & I^- s_\epsilon & I^- s_\kappa\end{bmatrix}\begin{bmatrix}\delta\varrho_1\\ \delta\varrho_2\\ \delta\varphi\\ \delta\psi\end{bmatrix}. \tag{14}$$

The parameters $G^\pm$, $H^\pm$ and $I^\pm$ are given as follows:

$$\begin{aligned} G^\pm &= \frac{\beta_c\varrho_1^{\mathrm{st}}}{\mathrm{s}_\epsilon - \mathrm{s}_\kappa}\left[\mathrm{s}_\epsilon\left(\mp\gamma_1/\gamma_2 - 1\right) + \mathrm{s}_\kappa\left(\mp\gamma_1/\gamma_2 + 1\right)\right],\\ H^\pm &= \frac{\beta_c\varrho_2^{\mathrm{st}}}{\mathrm{s}_\epsilon + \mathrm{s}_\kappa}\left[\mathrm{s}_\epsilon\left(\gamma_2/\gamma_1 \pm 1\right) + \mathrm{s}_\kappa\left(-\gamma_2/\gamma_1 \pm 1\right)\right],\\ I^\pm &= (\mathrm{s}_\epsilon - \mathrm{s}_\kappa)/\gamma_1 \pm (\mathrm{s}_\epsilon + \mathrm{s}_\kappa)/\gamma_2. \end{aligned} \tag{15}$$

For the $\mathcal{PT}$-symmetric case, eigenvalues ν of the dynamical matrix from Equation (14) are given as roots of the following polynomial:

$$\begin{gathered} \nu\left(\nu^3 + b\nu + c\right) = 0,\\ b = 4(\mathrm{c}_\epsilon + \mathrm{c}_\kappa)(\mathrm{c}_\epsilon\mathrm{s}_\kappa^2 + \mathrm{c}_\kappa\mathrm{s}_\epsilon^2)/\gamma^2, \quad c = -8\mathrm{s}_\epsilon\mathrm{s}_\kappa(\mathrm{c}_\epsilon + \mathrm{c}_\kappa)^2/\gamma. \end{gathered} \tag{16}$$

The eigenvalue $\nu_1 = 0$ is related to the freedom in determining, e.g., the phase ψ^{st} of a stationary state. Provided that $\mathrm{c}_\epsilon + \mathrm{c}_\kappa = 0$, we have $\nu_{1-4} = 0$ and Equation (13) gives us the trivial stationary state $\varrho_1^{\mathrm{st}} = \varrho_2^{\mathrm{st}} = 0$ lying on the border of stability.

Assuming $\mathcal{PT}$-symmetry and special case without $\chi^{(2)}$ interaction ($\kappa = 0$), we have $\mathrm{s}_\kappa = \mathrm{c}_\kappa = 0$ and the phase ψ^{st} is arbitrary. On the other hand, one solution for the remaining parameters of the stationary state is derived from Equations (12) and (13) for $\beta_c > 0$ in the following implicit form:

$$\mathrm{s}_\epsilon = \gamma, \quad \mathrm{c}_\epsilon = -\sqrt{\epsilon^2 - \gamma^2}, \quad \varrho_1^{\mathrm{st}} = \varrho_2^{\mathrm{st}} = \sqrt[4]{\epsilon^2 - \gamma^2}/\sqrt{\beta_c}. \tag{17}$$

Similarly, we reveal one stationary solution for $\beta_c < 0$:

$$\mathrm{s}_\epsilon = \gamma, \quad \mathrm{c}_\epsilon = \sqrt{\epsilon^2 - \gamma^2}, \quad \varrho_1^{\mathrm{st}} = \varrho_2^{\mathrm{st}} = \sqrt[4]{\epsilon^2 - \gamma^2}/\sqrt{-\beta_c}. \tag{18}$$

Eigenvalues of the dynamical matrix in Equation (14) are obtained for both solutions in Equations (17) and (18) as $\nu_{1-4} = 0$, i.e., the states are at the border of stability.

For nonzero κ, we first address the stationary states in EPs ($\mathcal{PT}$-symmetric case) for specific values of the phase $\psi^{\rm st}$. The trivial stationary states with $\varrho_1^{\rm st} = \varrho_2^{\rm st} = 0$ and zero eigenvalues $\nu_{1-4} = 0$ in the stability analysis are found under the conditions summarized in Table 1.

Table 1. Parameters of the trivial stationary states $\varrho_1^{\rm st} = \varrho_2^{\rm st} = 0$ with zero eigenvalues $\nu_{1-4} = 0$ for specific values of the phase $\psi^{\rm st}$.

$\psi^{\rm st} = 0$	$\mathrm{s}_\kappa = 0$	$\mathrm{c}_\kappa = \kappa$	$\mathrm{s}_\epsilon = \pm\gamma$	$\mathrm{c}_\epsilon = -\kappa$
$\psi^{\rm st} = \pi/2$	$\mathrm{s}_\kappa = \kappa$	$\mathrm{c}_\kappa = 0$	$\mathrm{s}_\epsilon = \pm\epsilon$	$\mathrm{c}_\epsilon = 0$
$\psi^{\rm st} = \pi$	$\mathrm{s}_\kappa = 0$	$\mathrm{c}_\kappa = -\kappa$	$\mathrm{s}_\epsilon = \pm\gamma$	$\mathrm{c}_\epsilon = \kappa$
$\psi^{\rm st} = 3\pi/2$	$\mathrm{s}_\kappa = -\kappa$	$\mathrm{c}_\kappa = 0$	$\mathrm{s}_\epsilon = \pm\epsilon$	$\mathrm{c}_\epsilon = 0$

The nontrivial stationary solution with $\varrho_1^{\rm st} = \varrho_2^{\rm st} = \sqrt{2\kappa/\beta_c}$ in EPs is revealed for $\psi^{\rm st} = \pi$ and $\beta_c > 0$:

$$\mathrm{s}_\kappa = 0, \;\; \mathrm{c}_\kappa = -\kappa, \;\; \mathrm{s}_\epsilon = \gamma, \;\; \mathrm{c}_\epsilon = -\kappa. \tag{19}$$

On the other hand, we have for $\beta_c < 0$ and $\psi^{\rm st} = 0$ the stationary solution with $\varrho_1^{\rm st} = \varrho_2^{\rm st} = \sqrt{2\kappa/(-\beta_c)}$ in EPs provided that

$$\mathrm{s}_\kappa = 0, \;\; \mathrm{c}_\kappa = \kappa, \;\; \mathrm{s}_\epsilon = \gamma, \;\; \mathrm{c}_\epsilon = \kappa. \tag{20}$$

Both solutions in Equations (19) and (20) have the same eigenvalues $\nu_{1,2} = 0$ and $\nu_{3,4} = \pm i2\sqrt{2}\kappa$ in the stability analysis, i.e., no amplification of amplitude fluctuations occur.

For an arbitrary phase $\psi^{\rm st}$, Equation (12) admits four possible values for the phase $\varphi^{\rm st}$:

$$\varphi_1^{\rm st} = \varphi_{\rm base}^{\rm st}, \;\; \varphi_2^{\rm st} = \pi - \varphi_{\rm base}^{\rm st}, \;\; \varphi_3^{\rm st} = \pi + \varphi_{\rm base}^{\rm st}, \;\; \varphi_4^{\rm st} = 2\pi - \varphi_{\rm base}^{\rm st}, \tag{21}$$

where $\varphi_{\rm base}^{\rm st} = \arcsin(\sqrt{\kappa^2 \sin^2(\psi^{\rm st}) + \gamma^2}/\epsilon)$. However, only some of them lead to real and nonnegative amplitudes $\varrho_1^{\rm st}$ and $\varrho_2^{\rm st}$ in Equation (13) and nonnegative expression in Equation (10). According to Equation (12), $|\mathrm{s}_\epsilon| \geq |\mathrm{s}_\kappa|$. Equation (12) can also be recast into the form suitable for the discussion:

$$\mathrm{c}_\epsilon^2 - \mathrm{c}_\kappa^2 = \epsilon^2 - \kappa^2 - \gamma^2. \tag{22}$$

Considering Equation (22) for $\epsilon^2 - \kappa^2 - \gamma^2 \geq 0$ we have $|\mathrm{c}_\epsilon| \geq |\mathrm{c}_\kappa|$. If $\beta_c > 0$ [$\beta_c < 0$], Equation (10) requires $\mathrm{c}_\epsilon \leq 0$ [$\mathrm{c}_\epsilon \geq 0$] and this admits the phases $\varphi_2^{\rm st}$ and $\varphi_3^{\rm st}$ [$\varphi_1^{\rm st}$ and $\varphi_4^{\rm st}$]. The expression (13) for $\varrho_1^{\rm st}$ requires $\mathrm{s}_\epsilon \geq 0$ independently of the sign of β_c and so only the phases $\varphi_1^{\rm st}$ and $\varphi_2^{\rm st}$ can be considered. Both conditions are fulfilled only for the phase $\varphi_2^{\rm st}$ [$\varphi_1^{\rm st}$] for $\beta_c > 0$ [$\beta_c < 0$].

On the other hand, we have $|\mathrm{c}_\epsilon| \leq |\mathrm{c}_\kappa|$ for $\epsilon^2 - \kappa^2 - \gamma^2 \leq 0$. In this case, $\mathrm{c}_\kappa \leq 0$ [$\mathrm{c}_\kappa \geq 0$] is needed in Equation (10) for $\beta_c > 0$ [$\beta_c < 0$] and so $\psi^{\rm st} \in \langle \pi/2, 3\pi/2 \rangle$ [$\psi^{\rm st} \in \langle 0, \pi/2 \rangle \cup \langle 3\pi/2, 2\pi \rangle$]. Similarly as above, $\mathrm{s}_\epsilon \geq 0$ guarantees nonnegative expression (13) for $\varrho_1^{\rm st}$ for arbitrary β_c, i.e., only the phases $\varphi_1^{\rm st}$ and $\varphi_2^{\rm st}$ are allowed. According to both conditions, nontrivial stationary states are expected for the phases $\varphi_1^{\rm st}$ and $\varphi_2^{\rm st}$ in the interval of phase $\psi^{\rm st} \in \langle \pi/2, 3\pi/2 \rangle$ [$\psi^{\rm st} \in \langle 0, \pi/2 \rangle \cup \langle 3\pi/2, 2\pi \rangle$] for $\beta_c > 0$ [$\beta_c < 0$].

The EPs occurring at the border of two above discussed regions need special attention. According to Equation (22), we have $|\mathrm{c}_\epsilon| = |\mathrm{c}_\kappa|$ at the EPs. The analysis reveals that on the top of the stationary states characterized in the above two paragraphs, the trivial stationary states with $\varrho_1^{\rm st} = \varrho_2^{\rm st} = 0$ exist for the phase $\varphi_3^{\rm st}$ in the interval $\psi^{\rm st} \in \langle 0, \pi/2 \rangle \cup \langle 3\pi/2, 2\pi \rangle$ and for the phase $\varphi_4^{\rm st}$ in the interval $\psi^{\rm st} \in \langle \pi/2, 3\pi/2 \rangle$ independently of the sign of β_c.

The above general conclusions are further illustrated in the graphs in Figure 1 where the stationary states and their stability are analyzed in the plane $(\gamma/\epsilon, \psi^{\rm st})$ for the case $\beta_c > 0$. In Figure 1, we characterize the stationary states by intensities $\varrho_1^{\rm st2}$ and $\varrho_2^{\rm st2}$ of modes 1 and 2, respectively. We judge

the stationary states according to the maximal values of imaginary and real parts of the complex frequencies ν_{1-4}. A positive (negative) imaginary part means amplification (attenuation) of amplitude fluctuations around the stationary state (we note the inverse notation for signs for ν and γ). A nonzero real part then indicates oscillations in the evolution of amplitude fluctuations. We have $\kappa/\epsilon = 0.5$ for the graphs drawn in Figure 1 and so the EP occurs for $\gamma_{\mathrm{EP}}/\epsilon = \sqrt{3}/2 \approx 0.87$. The stationary solutions for the phase φ_1^{st} exist only in the area with exponential increase of amplitudes ($\gamma \geq \gamma_{\mathrm{EP}}$), they are unstable and amplitude fluctuations oscillate. Only at the EP, the amplitudes ϱ_1^{st} and ϱ_2^{st} are zero and the state is at the border of stability. On the other hand, there exist stationary states for the phase φ_2^{st} in the oscillatory regime of amplitude evolution ($\gamma < \gamma_{\mathrm{EP}}$). According to the graph in Figure 1b amplitude fluctuations around these stationary states oscillate. They are amplified except for the line $\psi^{\mathrm{st}} = \pi$ that lies at the border of stability (see Figure 1d). According to the graphs in Figure 1e–h, the pattern of intensity ϱ_1^{st2} of mode 1 is a mirror image of the pattern of intensity ϱ_2^{st2} of mode 2 with respect to the plane $\psi^{\mathrm{st}} = \pi$ (compare Equation (13) for $\gamma_2 = -\gamma_1$ and $\pm \mathrm{s}_\kappa$).

The analysis of the graphs for the case with $\beta_c < 0$ drawn under the conditions of the graphs in Figure 1 reveals similarity provided that we replace φ_1^{st} by φ_2^{st}, shift the phase ψ^{st} by π and exchange mode amplitudes ϱ_1^{st} and ϱ_2^{st}. This similarity is illustrated in the graphs in Figure 2 where the stationary intensities and stability parameters are drawn at the EP for both cases. Considering $\beta_c > 0$ [$\beta_c < 0$] and following the graphs in Figure 2, there exist only the trivial stationary states with $\varrho_1^{\mathrm{st}} = \varrho_2^{\mathrm{st}} = 0$ at the border of stability for $\psi^{\mathrm{st}} \in \langle 0, \pi/2\rangle \cup \langle 3\pi/2, 2\pi\rangle$ [$\psi^{\mathrm{st}} \in \langle \pi/2, 3\pi/2\rangle$] and φ_2^{st} [φ_1^{st}]. For the remaining phases ψ^{st} nontrivial stationary states are found. These states are unstable except for the state with $\psi^{\mathrm{st}} = \pi$ [$\psi^{\mathrm{st}} = 0$] and φ_2^{st} [φ_1^{st}] that is at the border of stability and amplitude fluctuations around this state oscillate. Parameters for this state are given in Equation (19) (Equation (20)).

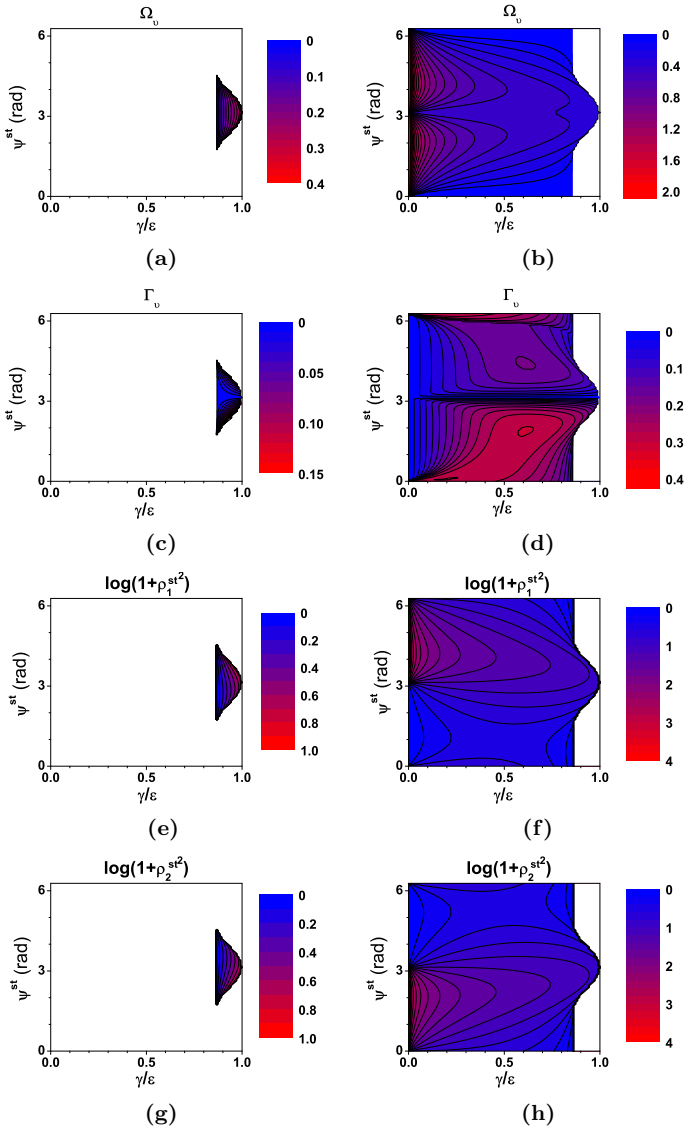

Figure 1. Maximal values of the real and imaginary parts of four complex frequencies ν in the stability analysis expressed via functions $\Omega_\nu = \log[1 + |\mathrm{Re}(\nu)|]$ (**a**,**b**) and $\Gamma_\nu = \mathrm{sign}[\mathrm{Im}(\nu)] \log[1 + |\mathrm{Im}(\nu)|]$ (**c**,**d**), respectively, and intensities ϱ_1^{st2} (**e**,**f**) and ϱ_2^{st2} (**g**,**h**) of modes 1 and 2, respectively, as they depend on dimensionless attenuation/amplification parameter γ/ϵ and phase ψ^{st} for stationary states with φ_1^{st} (**a**,**c**,**e**,**g**) and φ_2^{st} (**b**,**d**,**f**,**h**) defined in Equation (21); symbol sign gives the sign of the argument, log means the decimal logarithm, Re (Im) stands for the real (imaginary) part of the argument, $\kappa/\epsilon = 0.5$, and $\beta_c/\epsilon = 0.1$.

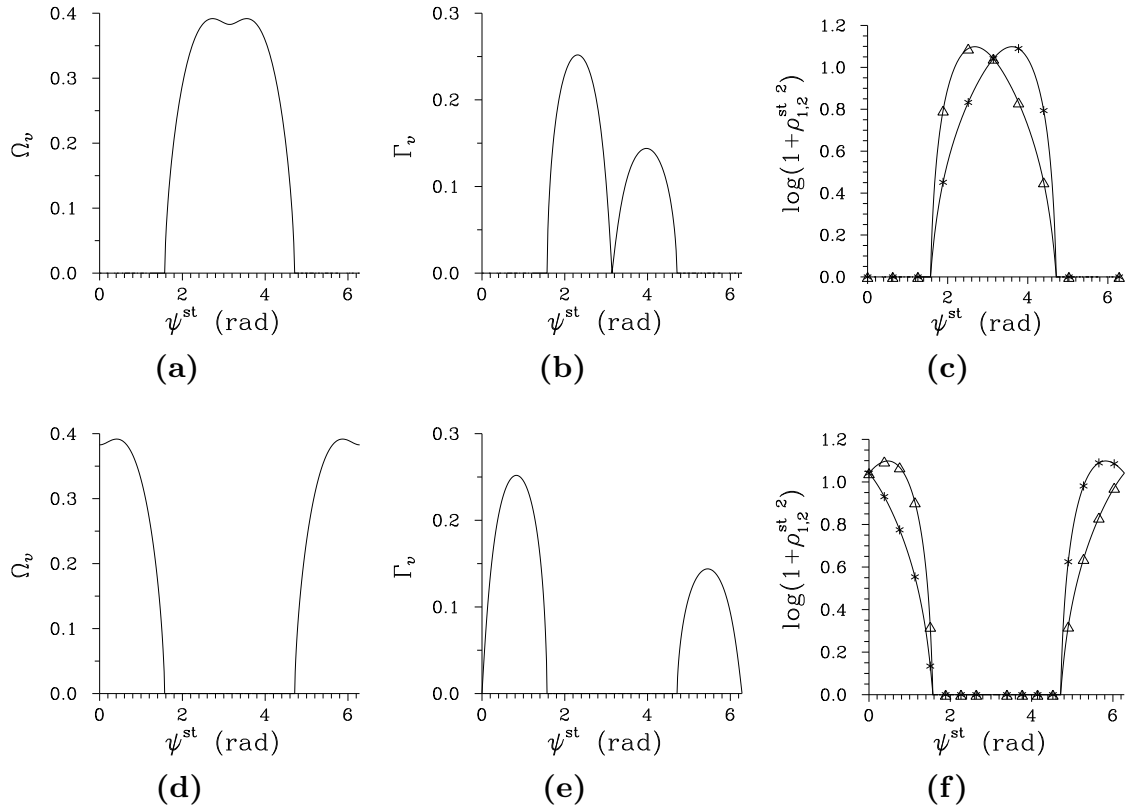

Figure 2. Maximal values of the real and imaginary parts of four complex frequencies ν in the stability analysis expressed by functions Ω_ν (**a**,**d**) and Γ_ν (**b**,**e**), respectively, and intensities $\varrho^{\mathrm{st}2}$ of mode 1 ($*$) and 2 ($\triangle$) (**c**,**f**) as they depend on phase ψ^{st} for φ_2^{st} (see Equation (21)) and $\beta_c/\epsilon = 0.1$ (**a**–**c**) and φ_1^{st} and $\beta_c/\epsilon = -0.1$ (**d**–**f**); EP condition $\gamma = \sqrt{\epsilon^2 - \kappa^2}$ is assumed. Functions Ω_ν and Γ_ν as well as the other parameters are given in the caption to Figure 1.

4. Quantum Properties of the Evolving States

We analyze the properties of states evolving from the stationary states determined above and compare them with those characterizing the states originating from non-stationary states. For an initial stationary state, the evolution is described by the Heisenberg equations in Equation (4) linearized around the initial complex amplitudes α_1^{st} and α_2^{st} ($\hat{a}_j = \alpha_j^{\mathrm{st}} + \delta\hat{a}_j$, $j = 1, 2$),

$$\begin{aligned}
\frac{d\delta\hat{a}_1}{dt} &= -\left(\gamma_1 + i\beta_c|\alpha_2^{\mathrm{st}}|^2\right)\delta\hat{a}_1 - i\left(\epsilon + \beta_c\alpha_1^{\mathrm{st}}\alpha_2^{\mathrm{st}*}\right)\delta\hat{a}_2 - i\left(\kappa + \beta_c\alpha_1^{\mathrm{st}}\alpha_2^{\mathrm{st}}\right)\delta\hat{a}_2^\dagger + \hat{l}_1, \\
\frac{d\delta\hat{a}_2}{dt} &= -i\left(\epsilon + \beta_c\alpha_1^{\mathrm{st}*}\alpha_2^{\mathrm{st}}\right)\delta\hat{a}_1 - i\left(\kappa + \beta_c\alpha_1^{\mathrm{st}}\alpha_2^{\mathrm{st}}\right)\delta\hat{a}_1^\dagger - \left(\gamma_2 + i\beta_c|\alpha_1^{\mathrm{st}}|^2\right)\delta\hat{a}_2 + \hat{l}_2,
\end{aligned} \tag{23}$$

and the Hermitian-conjugated ones. When an initial non-stationary state is assumed, we numerically solve the classical nonlinear Equations (6)–(9) and linearize the Heisenberg equations around the evolving complex amplitudes $\alpha_1(t)$ and $\alpha_2(t)$ [45]. In both cases the solution can be expressed in the following general form

$$\begin{aligned}
\begin{bmatrix} \delta\hat{a}_1(t) \\ \delta\hat{a}_2(t) \end{bmatrix} &= \mathbf{U}(t)\begin{bmatrix} \delta\hat{a}_1(0) \\ \delta\hat{a}_2(0) \end{bmatrix} + \mathbf{V}(t)\begin{bmatrix} \delta\hat{a}_1^\dagger(0) \\ \delta\hat{a}_2^\dagger(0) \end{bmatrix} + \begin{bmatrix} \hat{f}_1(t) \\ \hat{f}_2(t) \end{bmatrix}, \\
\begin{bmatrix} \hat{f}_1(t) \\ \hat{f}_2(t) \end{bmatrix} &= \int_0^t dt'\mathbf{U}(t-t')\begin{bmatrix} \hat{l}_1(t') \\ \hat{l}_2(t') \end{bmatrix} + \int_0^t dt'\mathbf{V}(t-t')\begin{bmatrix} \hat{l}_1^\dagger(t') \\ \hat{l}_2^\dagger(t') \end{bmatrix},
\end{aligned} \tag{24}$$

in which the matrices $\mathbf{U}(t)$ and $\mathbf{V}(t)$ and correlation functions of the fluctuating operator forces $\hat{f}_j(t)$, $j = 1, 2$, are determined numerically in general [45] and analytically under specific conditions [35,45].

We consider the initial vacuum state for the evolution of operator amplitude corrections. In this case, the evolving states remain Gaussian and so the following six correlation functions characterize them completely [22,35]:

$$\langle \delta\hat{a}_j^\dagger(t)\delta\hat{a}_j(t)\rangle, \;\; \langle [\delta\hat{a}_j(t)]^2\rangle, \;\; j = 1, 2, \;\; \langle \delta\hat{a}_1^\dagger(t)\delta\hat{a}_2(t)\rangle, \;\; \langle \delta\hat{a}_1(t)\delta\hat{a}_2(t)\rangle. \tag{25}$$

They are easily determined from Equation (24). All quantities characterizing the evolving states can then be expressed in terms of the correlation functions (25). For example, the principal squeeze variance of mode j is obtained as [49]

$$\lambda_j = 1 + 2\left[\langle \delta\hat{a}_j^\dagger(t)\delta\hat{a}_j(t)\rangle - |\langle [\delta\hat{a}_j(t)]^2\rangle|\right], \;\; j = 1, 2. \tag{26}$$

Determination of the covariance matrix in the symmetric operator ordering then allows to reach the logarithmic negativity E_N that is a suitable quantifier of the entanglement between the modes (for details, see [50,51]).

In Figure 3, we compare the state evolution around a stationary state with that occurring around a non-stationary state. As a stationary state, we consider the state given in Equation (19). The analyzed non-stationary state evolves from the state that differs from that in Equation (19) in the phase $\psi^{\rm init} = 0$:

$$\mathrm{s}_\kappa^{\rm init} = 0, \;\; \mathrm{c}_\kappa^{\rm init} = \kappa, \;\; \mathrm{s}_\epsilon^{\rm init} = -\gamma, \;\; \mathrm{c}_\epsilon^{\rm init} = \kappa. \tag{27}$$

For the stationary state that lies at the border of stability, both intensities $\varrho_1^2(t)$ and $\varrho_2^2(t)$ increase during the evolution and the fluctuating forces give dominant contribution to this increase (compare solid and dashed curves in Figure 3a). Contrary to this, for the initial non-stationary state the intensity $\varrho_1^2(t)$ of attenuated mode 1 first considerably decreases whereas the intensity $\varrho_2^2(t)$ of amplified mode 2 increases constantly. According to the curves in Figure 3d, the relative contribution of fluctuating forces to the dynamics of intensities is small. In both cases, only the attenuated mode 1 exhibits squeezing (for the principal squeeze variances $\lambda_{1,2}$, see Figure 3b,e) and both modes are entangled (for the logarithmic negativity E_N, see Figure 3c,f) for a limited time period. It is worth noting that both squeezing and entanglement are stronger for the initial non-stationary state. The comparison of curves in Figure 3b,d for the principal squeeze variances $\lambda_{1,2}$ and in Figure 3c,e for the logarithmic negativity E_N drawn with and without the inclusion of fluctuating forces clearly documents substantial role of these forces in consistent description of $\mathcal{PT}$-symmetric quantum systems.

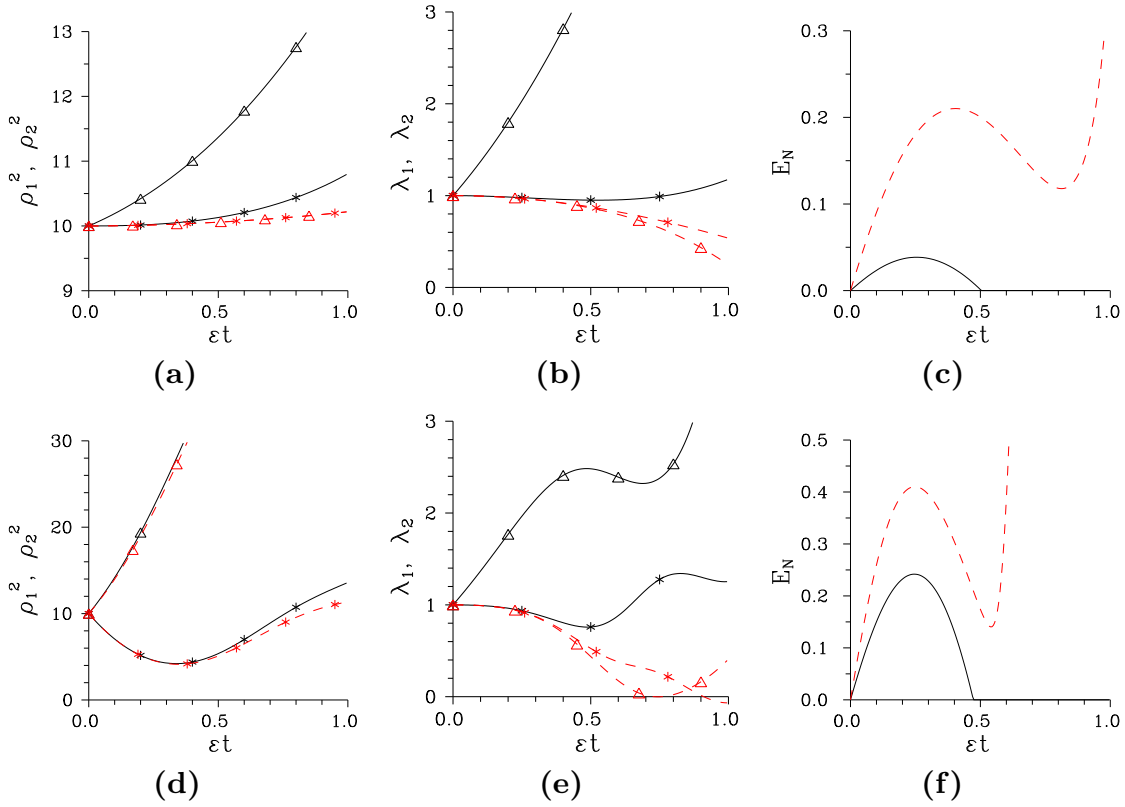

Figure 3. Intensities ϱ^2 (**a**,**d**) and principal squeeze variances λ of mode 1 ($*$) and 2 ($\triangle$) (**b**,**e**) and logarithmic negativity E_N (**c**,**f**) as they evolve along dimensionless time ϵt for initial stationary (non-stationary) state with $\psi^{\rm st} = \pi$ [$\psi^{\rm init} = 0$], $\varrho_{1,2} = \sqrt{2\kappa/\beta_c}$ and $\varphi_2^{\rm st}$ (**a**–**c**) [$\varphi_4^{\rm init}$ (**c**–**e**)] given in Equation (19) (Equation (27)), assuming $\gamma = \sqrt{\epsilon^2 - \kappa^2}$, $\kappa/\epsilon = 0.5$, and $\beta_c/\epsilon = 0.1$. The initial vacuum state is assumed, evolution is treated with [without] fluctuating forces (black solid [red dashed] curves).

5. Conclusions

Two oscillator modes with balanced attenuation and amplification were considered to be mutually coupled via the usual linear coupling, $\chi^{(2)}$ parametric process and cross-Kerr nonlinearity. Nontrivial stationary states that occur owing to the cross-Kerr nonlinearity were identified and their stability was determined. The stationary states typically form one-parameter systems. There occur only unstable stationary states and states lying at the border of stability (zero imaginary parts of frequencies in the stability analysis). The solution of linearized operator equations for mode amplitudes around these stationary states revealed nonclassical properties of the evolving states (single-mode squeezing, entanglement). Initial non-stationary states seem to be more suitable for nonclassical-state generation than the stationary ones at the border of stability. Substantial role of the fluctuating Langevin operator forces in consistent description of the system was demonstrated.

Author Contributions: Conceptualization, J.P.J. and A.L.; Investigation, J.P.J. and A.L.; Software, J.P.J.; Writing—original draft, J.P.J.; Writing—review & editing, J.P.J. and A.L.

Funding: J.P. acknowledges the support by the GA ČR project 18-22102S. A.L. gratefully acknowledges the support from the project IGA_PrF_2019_008 of Palacký University.

Acknowledgments: The authors thank J. K. Kalaga and W. Leoński for discussions about PT-symmetry and Kerr effect.

Conflicts of Interest: The authors declare no conflict of interest.

References

1. Bender, C.M.; Boettcher, S. Real Spectra in non-Hermitian Hamiltonians Having $\mathcal{PT}$ Symmetry. *Phys. Rev. Lett.* **1998**, *80*, 5243–5246. [CrossRef]
2. Bender, C.M.; Boettcher, S.; Meisinger, P.N. $\mathcal{PT}$-symmetric quantum mechanics. *J. Math. Phys.* **1999**, *40*, 2201–2229. [CrossRef]
3. Bender, C.M.; Brody, D.C.; Jones, H.F. Must a Hamiltonian be Hermitian? *Am. J. Phys.* **2003**, *71*, 1095–1102. [CrossRef]
4. Morales, J.D.H.; Guerrero, J.; López-Aguayo, S.; Rodríguez-Lara, B.M. Revisiting the Optical $\mathcal{PT}$-symmetric Dimer. *Symmetry* **2016**, *8*, 83. [CrossRef]
5. Meystre, P.; Sargent, M., III. *Elements of Quantum Optics*, 4th ed.; Springer: Berlin, Germany, 2007.
6. Sargent, M.; Scully, M.O.; Lamb, W.E. *Laser Physics*; Addison-Wesley: Boston, MA, USA, 1974.
7. El-Ganainy, R.; Makris, K.G.; Christodoulides, D.N.; Musslimani, Z.H. Theory of coupled optical $\mathcal{PT}$-symmetric structures. *Opt. Lett.* **2007**, *32*, 2632–2634. [CrossRef] [PubMed]
8. Ramezani, H.; Kottos, T.; El-Ganainy, R.; Christodoulides, D.N. Unidirectional nonlinear $\mathcal{PT}$-symmetric optical structures. *Phys. Rev. A* **2010**, *82*, 043803. [CrossRef]
9. Zyablovsky, A.A.; Vinogradov, A.P.; Pukhov, A.A.; Dorofeenko, A.V.; Lisyansky, A.A. $\mathcal{PT}$-symmetry in optics. *Phys.-Uspekhi* **2014**, *57*, 1063–1082. [CrossRef]
10. Ögren, M.; Abdullaev, F.K.; Konotop, V.V. Solitons in a $\mathcal{PT}$-symmetric $\chi^{(2)}$ coupler. *Opt. Lett.* **2017**, *42*, 4079–4082. [CrossRef]
11. Turitsyna, E.G.; Shadrivov, I.V.; Kivshar, Y.S. Guided modes in non-Hermitian optical waveguides. *Phys. Rev. A* **2017**, *96*, 033824. [CrossRef]
12. Xu, X.; Shi, L.; Ren, L.; Zhang, X. Optical gradient forces in $\mathcal{PT}$-symmetric coupled-waveguide structures. *Opt. Express* **2018**, *26*, 10220–10229. [CrossRef]
13. Liu, Z.P.; Zhang, J.; Özdemir, S.K.; Peng, B.; Jing, H.; Lü, X.Y.; Li, C.W.; Yang, L.; Nori, F.; Liu, Y.X. Metrology with $\mathcal{PT}$-Symmetric Cavities: Enhanced Sensitivity near the $\mathcal{PT}$-Phase Transition. *Phys. Rev. Lett.* **2016**, *117*, 110802. [CrossRef] [PubMed]
14. Zhou, X.; Chong, Y.D. $\mathcal{PT}$ symmetry breaking and nonlinear optical isolation in coupled microcavities. *Opt. Express* **2016**, *24*, 6916–6930. [CrossRef] [PubMed]
15. Arkhipov, I.I.; Miranowicz, A.; Di Stefano, O.; Stassi, R.; Savasta, S.; Nori, F.; Özdemir, S.K. Scully-Lamb quantum laser model for parity-time-symmetric whispering-gallery microcavities: Gain saturation effects and nonreciprocity. *Phys. Rev. A* **2019**, *99*, 053806. [CrossRef]
16. Graefe, E.M.; Jones, H.F. $\mathcal{PT}$-symmetric sinusoidal optical lattices at the symmetry-breaking threshold. *Phys. Rev. A* **2011**, *84*, 013818. [CrossRef]
17. Miri, M.A.; Regensburger, A.; Peschel, U.; Christodoulides, D.N. Optical mesh lattices with $\mathcal{PT}$ symmetry. *Phys. Rev. A* **2012**, *86*, 023807. [CrossRef]
18. Ornigotti, M.; Szameit, A. Quasi $\mathcal{PT}$-symmetry in passive photonic lattices. *J. Opt.* **2014**, *16*, 065501. [CrossRef]
19. Shui, T.; Yang, W.X.; Li, L.; Wang, X. Lop-sided Raman-Nath diffraction in $\mathcal{PT}$-antisymmetric atomic lattices. *Opt. Lett.* **2019**, *44*, 2089–2092. [CrossRef]
20. Tchodimou, C.; Djorwe, P.; Nana Engo, S.G. Distant entanglement enhanced in $\mathcal{PT}$-symmetric optomechanics. *Phys. Rev. A* **2017**, *96*, 033856. [CrossRef]
21. Wang, D.Y.; Bai, C.H.; Liu, S.; Zhang, S.; Wang, H.F. Distinguishing photon blockade in a $\mathcal{PT}$-symmetric optomechanical system. *Phys. Rev. A* **2019**, *99*, 043818. [CrossRef]
22. Peřina, J. *Quantum Statistics of Linear and Nonlinear Optical Phenomena*; Kluwer: Dordrecht, The Netherlands, 1991.
23. Agarwal, G.S.; Qu, K. Spontaneous generation of photons in transmission of quantum fields in $\mathcal{PT}$-symmetric optical systems. *Phys. Rev. A* **2012**, *85*, 31802(R). [CrossRef]
24. Scheel, S.; Szameit, A. $\mathcal{PT}$-symmetric photonic quantum systems with gain and loss do not exist. *Eur. Phys. Lett.* **2018**, *122*, 34001. [CrossRef]
25. Peřinová, V.; Lukš, A.; Křepelka, J. Quantum description of a $\mathcal{PT}$-symmetric nonlinear directional coupler. *J. Opt. Soc. Am. B* **2019**, *36*, 855–861. [CrossRef]
26. Antonosyan, D.A.; Solntsev, A.S.; Sukhorukov, A.A. Photon-pair generation in a quadratically nonlinear parity-time symmetric coupler. *Phot. Res.* **2018**, *6*, A6–A9. [CrossRef]

27. Naikoo, J.; Thapliyal, K.; Banerjee, S.; Pathak, A. Quantum Zeno effect and nonclassicality in a $\mathcal{PT}$-symmetric system of coupled cavities. *Phys. Rev. A* **2019**, *99*, 023820. [CrossRef]
28. Miranowicz, A.; Leoński, W. Two-mode optical state truncation and generation of maximally entangled states in pumped nonlinear couplers. *J. Phys. B At. Mol. Opt. Phys.* **2006**, *39*, 1683–1700. [CrossRef]
29. He, B.; Yan, S.B.; Wang, J.; Xiao, M. Quantum noise effects with Kerr-nonlinearity enhancement in coupled gain-loss waveguides. *Phys. Rev. A* **2015**, *91*, 053832. [CrossRef]
30. Kalaga, J.K.; Kowalewska-Kudłaszyk, A.; Leoński, W.; Barasinski, A. Quantum correlations and entanglement in a model comprised of a short chain of nonlinear oscillators. *Phys. Rev. A* **2016**, *94*, 032304. [CrossRef]
31. Vashahri-Ghamsari, S.; He, B.; Xiao, M. Continuous-variable entanglement generation using a hybrid $\mathcal{PT}$-symmetric system. *Phys. Rev. A* **2017**, *96*, 033806. [CrossRef]
32. Mandel, L.; Wolf, E. *Optical Coherence and Quantum Optics*; Cambridge University Press: Cambridge, UK, 1995.
33. Boyd, R.W. *Nonlinear Optics*, 2nd ed.; Academic Press: New York, NY, USA, 2003.
34. Peřina, J., Jr. Coherent light in intense spatiospectral twin beams. *Phys. Rev. A* **2016**, *93*, 063857. [CrossRef]
35. Peřina J., Jr.; Peřina, J. Quantum statistics of nonlinear optical couplers. In *Progress in Optics*; Wolf, E., Ed.; Elsevier: Amsterdam, The Netherlands, 2000; Volume 41, pp. 361–419.
36. Thapliyal, K.; Pathak, A.; Sen, B.; Peřina, J. Higher-order nonclassicalities in a codirectional nonlinear optical coupler: Quantum entanglement, squeezing, and antibunching. *Phys. Rev. A* **2014**, *90*, 013808. [CrossRef]
37. Sanders, B.C.; Milburn, G.J. Complementarity in a quantum nondemolition measurement. *Phys. Rev. A* **1989**, *39*, 694–702. [CrossRef] [PubMed]
38. Leoński, W.; Kowalewska-Kudlaszyk, A. Quantum Scissors and Finite-Dimensional States Engineering. In *Progress in Optics*; Wolf, E., Ed.; Elsevier: Amsterdam, The Netherlands, 2011; Volume 56, pp. 131–185.
39. Kalaga, J.K.; Jarosik, M.W.; Szczęśniak, R.; Nguen, T.D.; Leoński, W. Pulsed Nonlinear Coupler as an Effective Tool for the Bell-Like States Generation. *Acta Phys. Polon. A* **2019**, *135*, 273–275. [CrossRef]
40. Kalaga, J.K.; Kowalewska-Kudłaszyk, A.; Jarosik, M.W.; Szczęśniak, R.; Leoński, W. Enhancement of the entanglement generation via randomly perturbed series of external pulses in a nonlinear Bose-Hubbard dimer. *Nonlinear Dyn.* **2019**. [CrossRef]
41. Korolkova, N.; Peřina, J. Kerr nonlinear coupler with varying linear coupling coefficient. *J. Mod. Opt.* **1997**, *44*, 1525–1534. [CrossRef]
42. Fiurášek, J.; Křepelka, J.; Peřina, J. Quantum-phase properties of the Kerr couplers. *Opt. Commun.* **1999**, *167*, 115–124. [CrossRef]
43. Ariunbold, G.; Peřina, J. Non-classical behaviour and switching in Kerr nonlinear couplers. *J. Mod. Opt.* **2001**, *48*, 1005–1019. [CrossRef]
44. Bartkowiak, M.; Wu, L.A.; Miranowicz, A. Quantum circuits for amplification of Kerr nonlinearity via quadrature squeezing. *J. Phys. B At. Mol. Opt. Phys.* **2014**, *47*, 145501. [CrossRef]
45. Peřina, J., Jr.; Lukš, A.; Kalaga, J.; Leoński, W.; Miranowicz, A. Nonclassical light in quantum $\mathcal{PT}$-symmetric two-mode systems. To be published.
46. Sukhorukov, A.A.; Xu, Z.; Kivshar, Y.S. Nonlinear suppression of time reversals in $\mathcal{PT}$-symmetric optical couplers. *Phys. Rev. A* **2010**, *83*, 043818. [CrossRef]
47. Callen, H.B.; Welton, T.A. Irreversibility and Generalized Noise. *Phys. Rev.* **1951**, *83*, 34–40. [CrossRef]
48. Kubo, R. The fluctuation-dissipation theorem. *Rep. Prog. Phys.* **1966**, *29*, 255–284. [CrossRef]
49. Lukš, A.; Peřinová, V.; Peřina, J. Principal squeezing of vacuum fluctuations. *Opt. Commun.* **1988**, *67*, 149–151. [CrossRef]
50. Hill, S.; Wootters, W.K. Computable entanglement. *Phys. Rev. Lett.* **1997**, *78*, 5022. [CrossRef]
51. Adesso, G.; Illuminati, F. Entanglement in continuous variable systems: Recent advances and current perspectives. *J. Phys. A Math. Theor.* **2007**, *40*, 7821–7880. [CrossRef]